

MOX–Report No. 17/2009

3D Inverse and Direct Structural Modeling Workflow

MATTEO LONGONI, CORRADO MAGISTRONI,
PAOLO RUFFO, GIOVANNI SCROFANI

MOX, Dipartimento di Matematica “F. Brioschi”
Politecnico di Milano, Via Bonardi 9 - 20133 Milano (Italy)

mox@mate.polimi.it

<http://mox.polimi.it>

3D Inverse and Direct Structural Modeling Workflow

Matteo Longoni¹, Corrado Magistroni², Paolo Ruffo², Giovanni Scrofani²

May 12, 2009

¹ MOX– Modellistica e Calcolo Scientifico, Dipartimento di Matematica “F. Brioschi”,
Politecnico di Milano, Italy

² ENI S.p.A., E&P Division, Basin Geology Department, San Donato Milanese, Milan,
Italy

Keywords: Geological Modelling, Data Processing.

Abstract

The description and the interpretation of the geological evolution of sedimentary basins has recently received a great support from the use of mathematical models and numerical methods, taking advantage of more advanced hardware, both in graphic and computing power. We have developed a geological modeling workflow, based on GOCAD, for the 3D inverse and direct structural modeling of sedimentary basins. The workflow is based on an appropriate number of time-steps of restoration modeling coupled with forward/evolution modeling. During each step a GOCAD geological model provides support for data managing, pre- and post-processing for numerical solvers and the necessary interpretative model editing.

The capability of capturing and describing all the geometrical and structural features of an accurate geological model, leads to remarkable results in integrating available data, in validating restoration models and in reconstructing a reliable evolution of a basin.

The model is built with GOCAD, starting from the basin geometrical data. Topological complexities such as faulted stratified layers and salt diapirs are easily handled in a three-dimensional unstructured framework. Then the geometrical model is enriched with its physical properties, coming from seismic, well and field data and from the modeller conceptual model. The domain is then described with a user-defined tetrahedral mesh, necessary for the numerical simulation of its geological evolution. The output results, for example the updated position of horizon and fault surfaces, and the distributions in the domain of physical quantities such as stresses and displacements, are then imported in GOCAD by means of a fully-automatic procedure, for data visualization and analysis. The workflow can be iterated starting from the last updated configuration.

We present the application of the workflow to the simulation of the dynamic structural evolution in two realistic cases: a multi-faulted system and a diapir growth in a multi-layered sedimentary basin.

Introduction

The motivation that moves the study and the implementation of efficient and functional procedures for pre- and post-processing resides in the importance of having powerful and automatic tools for geological modeling and visualization of a huge quantity of data in a clear and effective layout.

The procedure we present in this work is intended to support the modeller for restoration, that is one of the existing techniques for obtaining an accurate and consistent interpreted geological section from seismic or well data. In particular we refer to the direct approach, by which the geological history is reconstructed from the past to nowadays in a forward evolution time direction. (for an overview on cross-section balancing and restoration techniques see [1]). Its main purpose is to verify the structural interpretation and geometry of a geological formation, and to validate models.

The appearance of CAD software for geological modeling has lead to a significant improvement in this research field, as the capturing of all the complex three-dimensional geometrical features assumes vital importance in comprehending earth movement and dynamics. On the other hand, in the petroleum industry, the representation, visualization and analysis of physical data is a key point in planning well drilling and in basin inspection, to reduce the risks of exploration.

The use of GOCAD coupled to a powerful dynamic solver represents an improvement step towards the simulation of the very true evolution of the dynamics of real three-dimensional sedimentary basins (see for example [2] and [3]). Indeed it allows the handling of geometrical tools for the structural modeling of geological objects in a three-dimensional framework, together with built-in algorithm for data processing and visualization. We exploit these resources to plan a procedure that is able, starting from a set of initial data, to build a structural model of stratified sedimentary basins for dynamic simulations, endowed with a tetrahedral mesh accounting of topological complexities. After the numerical simulations, the physical and geometrical results can be imported in GOCAD, for data visualization and surface reconstruction, for the inverse construction of the structural model.

The paper is organized as follows. In the first Section we present the structural modeling workflow applied to a stratified multi-faulted system together with an automatic proceeding for data visualization, focusing on the direct approach. In Section 2 we show a second significant case, a diapir growth, illustrating the model creation steps and the data visualization possibilities, and the surfaces reconstruction sequence that leads to the updated model, as an example of inverse approach. Finally, future works and developments are discussed.

1 Structural Modeling Workflow

The structural modeling workflow we propose aims at building a complete procedure for restoration pre- and post processing. We propose two sequences of steps that starting from horizon and fault surfaces are able to build in GOCAD a 3D structural model, to visualize the results of numerical simulation, and to update the structural configuration. We neglect here the seismic data analysis the input data come from, and we assume to already have horizons and faults available, in any GOCAD format.

The key features of the procedures are the capability of handling models of complex topology and the minimization of the user intervention in the post-processing phase, that is fully automatic. In the following we present the modeling of a sedimentary basin composed of three layers and in presence of two faults, that is shown in Figure 1. We exploit the StructuralModeling built-in GOCAD workflow and the Finite Element Mesh Constructor GOCAD module, respectively to define the domain boundaries and surfaces, and to create the mesh.

1.1 Pre-Processing

As we have previously said, the input data consist on the discretized surfaces of the basin. Though these can be represented in any GOCAD object, for example as *2D-Grid* or *PointsSets*, we suppose for simplicity they are available in the *Surface* format, as this is the most generic object and easily handled by the



Figure 1: The starting point of the pre-processing procedure: the surfaces representing the horizons (green, magenta and white) and the faults (red) are available in the GOCAD format *Surface*. The region we consider is highlighted in black. In this figure and in the following figures of this section, the view is expanded by a factor 2 in the Z direction.

processing tools we are going to use (anyway, it is always possible to convert or to extract a surface from those objects). The initial configuration then looks like the one shown in Figure 1. The procedure can be schematically sketched as follows:

1. set the walls of the domain of interest, exploiting the StructuralModeling workflow;
2. build a *Model3D* object representing the structural framework;
3. create the tetrahedral mesh, through a 1D and 2D intermediate meshes;
4. provide the structural model with properties.

In the following, all these steps are explained in details.

1.1.1 Domain of interest

We firstly define the region of interest from the available data. We exploit the first steps of the StructuralModeling workflow to characterize geologically the surfaces and to create the domain walls, choosing the top, the basement and the area of interest. It is also possible to rebuild the surfaces to fit the domain boundaries or to respect a mesh size. At this stage we do not care of the surface meshes, as they will be specifically considered later in the mesh generation process. Faults and horizons mutual contacts can be either modeled or not, depending on the approach of the solver. The resulting model is shown in Figure 2. The top is still fictitious here, as we are going to consider the actual top (green surface). The basement is chosen to conserve the original salt

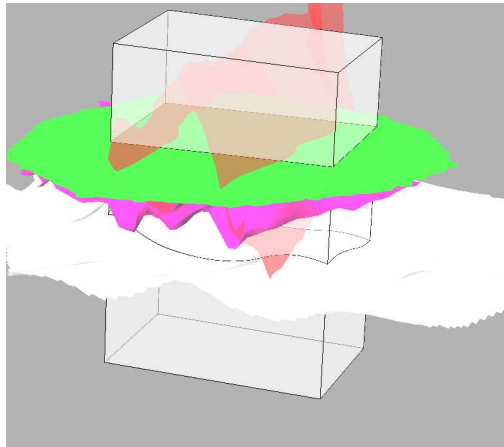


Figure 2: The application of the Structural Modeling workflow: the model is enriched with the delimiting walls, that define the volume of interest. In this case we do not model the horizon–fault contacts.

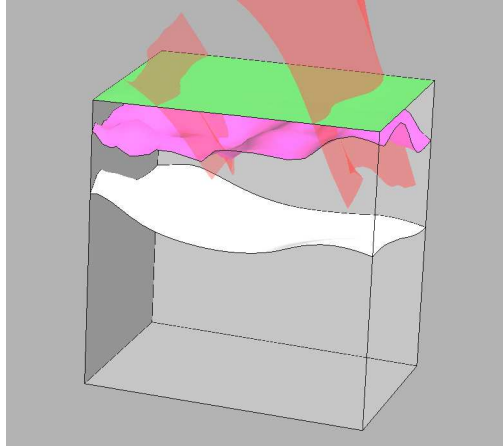


Figure 3: The model in the *Model3d* object. The faults are shown in red, but not explicitly included as surfaces in the *Model3d*.

volume (white surface and underlying layer) according to restoration data. All the objects are now *Surface* objects.

1.1.2 Structural Frame

From the previous data processing, we build the structural layout of the model, which is composed of all the intersection lines between surfaces. It is important to obtain a watertight frame, in order to preserve the proper subdivision of layers and subdomains. We create then a *Model3d* object, that exploits the algorithm described in [4] to guarantee the surfaces to intersect each other correctly, and hence to generate well-sealed regions. The *Model3d* is the recommended object as it the most rigorous way to associate a macro-topological model and a tessellated volume (see [5]). Indeed, it is the natural input of the tessellation tools and predisposed to the generation of a tetrahedral mesh over a structural model.

The surfaces to be included in the *Model3d* are in theory both the horizons and the faults of interest. Instead, here we do not include faults as they are modeled in a way that does not imply an explicit geometric representation in the structural framework. It depends however on the solver approach. The result is shown in Figure 3, where we have already removed the upper layer to obtain the actual top surface.

1.1.3 Mesh generation process

The volume tessellation is generated with the help of the GOCAD Tessellation workflow routines. By means of a process involving three sequential meshes, a 3D tetrahedral unstructured grid is built over the computational domain. To correctly discretize the model, this volume mesh should be conformal to both

external and internal surfaces. This task is accomplished by the method described in [6], that neglects any previous triangulation on surfaces and generates a mesh that respects the geometry of internal boundaries. It also implements algorithms for elements quality improvement.

Initially a 1D discretization is built on the radial lines composing the *Model3d* framework. Then, starting from this one-dimensional mesh, a 2D triangulation is constructed on every surface of the model, and hence the 3D tetrahedral discretization. In each step, refinement and adaptation tools are available to size the meshes on specific fitting requirements. In our case, we choose a constant 1D discretization for the frame, whose size is established to have a reasonable number of segments (and consequently triangles and tetrahedra) in the Z direction. As regards the 2D grid, two different constant sizes have been considered respectively for horizons and boundaries, to balance the global number of unknowns (that depends on the number of mesh nodes and elements) and the resolution desired. Finally an isotropic tetrahedral distribution is imposed for the volume discretization. The three resulting meshes are shown in Figure 4.

A remarkable feature is that the absence of faults in the geometric representation strongly simplifies the mesh generation process and increments the overall quality. In Figure 4(d) an example of anisotropic refinement is shown, that may be useful in specific applications. The tessellation is stored in a G \circ CAD object *Solid*, which contains also the *Model3d* and the surfaces.

1.1.4 Property modeling

The structural model can be endowed with additional informations, such as the physical properties of each layer or the boundary condition for the numerical simulation, that characterize it from the modellistic point of view. Among the possible categories and types, these features are applied as user-defined *Properties* on the object *Solid*, and through its internal objects *Surfaces*, they can be defined on either the whole domain or only on the boundary. This last case is the one shown in Figure 5(a), where a qualitative velocity distribution imposed only on the lateral walls is displayed. In our example, each boundary condition is initially applied on every wall by means of a flag property; then through flag-value defined regions their numerical values are assigned to the model, according to flags and regions. In terms of G \circ CAD *Properties*, each velocity component is an *Element* of a three-element property representing the vectorial velocity.

A particular kind of property that we impose is a distance function to indicate faults. In other words, faults are included in the model indirectly, by means of a node-related distance function, that measures the distance between a grid node and a fault surface (see Figure 5(b)). The fault region can be then identified by those nodes whose distance is lower than a user-defined threshold. It is worth noting that to capture the faults correctly, the grid size in this region should have the same order of magnitude of the fault thickness (that is about tens of meters), that may suggest the reference size for the tetrahedral

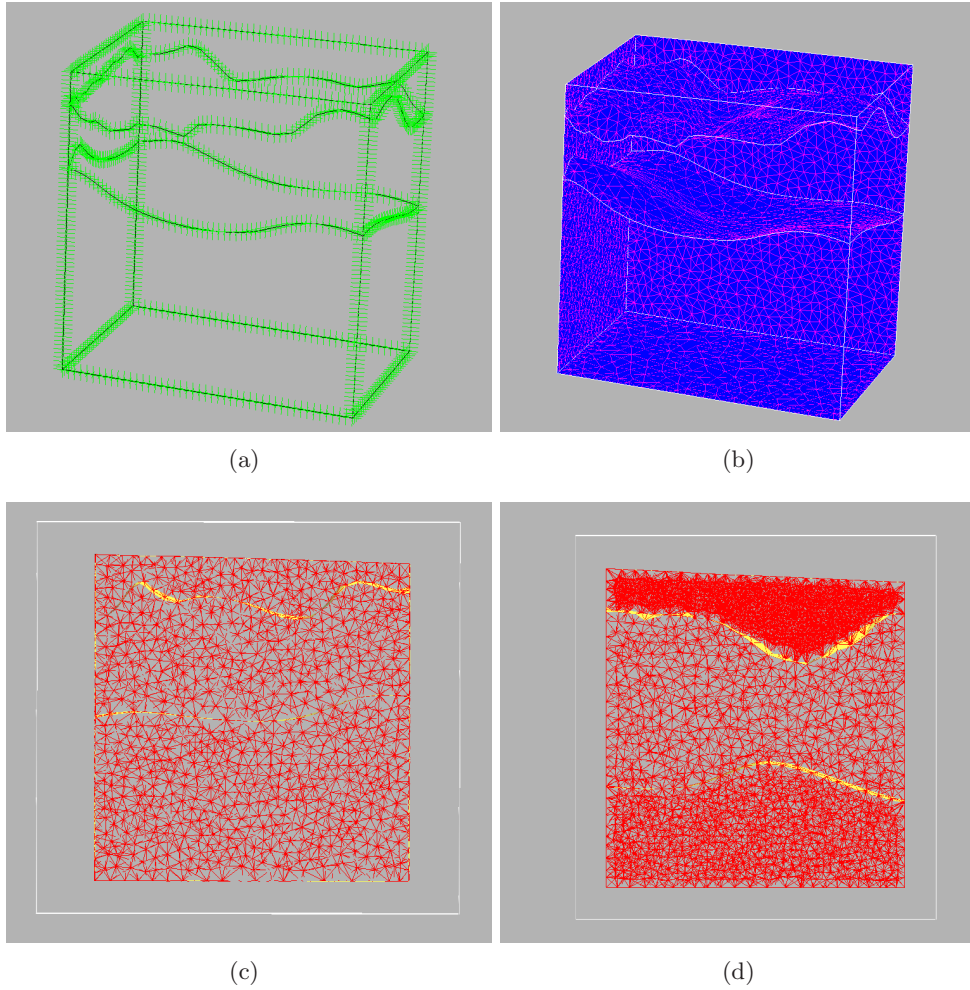


Figure 4: The mesh generation process: (a) the constant 1D discretization, with a compressive $Z_factor = 2$. (b) The 2D mesh in an open view of the model, with two different levels of uniform refinement for horizons and domain lateral boundaries. (c) The volume mesh: the reference size is chosen to discretize the thinnest subdomain with at least two layers of tetrahedra, to preserve accuracy. (d) An example of anisotropic refinement: a constant subdomain-dependent size is prescribed for the tetrahedra refinement.

refinement. Unfortunately this is usually much smaller than the basin dimension (of the order of tens or hundreds of kilometres), and would lead to over-refined meshes. For this reason dedicated refinement algorithms may be required (see for example [7]).

The structural workflow is then completed. The whole model is saved in the

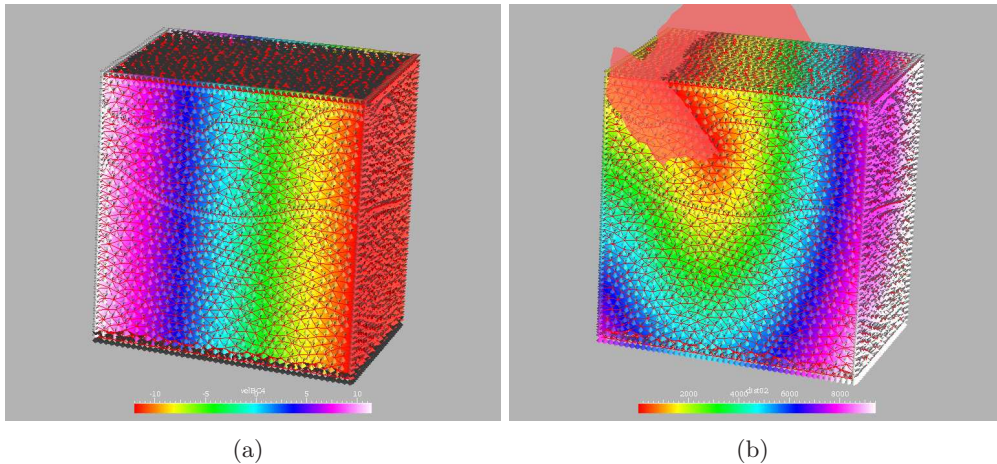


Figure 5: Examples of property definition. (a) The distribution of the X-component of the extension velocity of the basin, defined on the grid nodes as a linear function of the position along the X axis, and only over the lateral boundaries (the nodes where the property is not defined are displayed in black). (b) Example of fault modeling through a distance function, that identifies the region of the model crossed by one fault (red surface).

Solid output file, that contains all the physical, mathematical and geometrical informations required. These can be finally extracted and formatted for the numerical solver.

1.2 Post-Processing

The post-processing procedure focuses on data visualization and surfaces reconstruction. It strongly relies upon the Discrete Smooth Interpolation, introduced and developed in [8] and [9], that is used for interpolating both data and surfaces. The procedure benefits from a script of GOCAD CliCommands to manage automatically all the available output data. In our case these can be divided into two main categories: we have scalar or vectorial fields of physical quantities (such as velocity, stress, pressure, density, ...), where each component is a property of a GOCAD *PointsSet* object, and the model surfaces and boundaries, that are printed out directly in the *Surface* format or as sets of points clouds. In the first case each property is attached to the nodes of the related mesh, and the procedure interpolates them through the DSI on a three-dimensional domain, and paints a *Voxel* object for visualization. In the latter, a sequence of steps has been developed to reconstruct the actual surface by means of the DSI as a compromise between data fitting and function smoothness. This last feature in particular is suitable for updating the model configuration and restart the simulation every time the numerical solver is not able to handle a topological

change or geological event that may occur. In particular the two proceedings consist in the following steps:

- | <u>Data Visualization</u> | <u>Surface Reconstruction</u> |
|---|---|
| 1. Load the property and the related mesh | 1. Load the dataset containing the surface point |
| 2. Create a <i>Voxel</i> | 2. Build a constrained border and surface |
| 3. Interpolate the property on the <i>Voxel</i> | 3. Run a sequence of alternate isotropic DSI for surface smoothing and data fitting |

We would like to remark that the procedure is fully automatic, that is each step can be performed without any user intervention. On the other hand, to modify and customize the proposed post-processing settings (for example the number of cycles of the DSI), it suffices for the user to edit the file scripts, and to set the desired parameters. In any case, the scripts can be then run automatically.

In the following figures some results are presented. The basin dimension are $13.8 \times 9.2 \times 7.1$ km, and the mesh is made of 19210 points and 96428 tetrahedra, for a simulation step lasting 7 million of years.

We show in Figure 6 three examples of property visualization, in particular the module of the velocity, the S_{ZZ} stress component and the viscosity distributions on a section crossing the faults. In all the plots, faults are clearly visible, as high-speed, low-stress and low-viscosity regions. In Figure 7 the surface reconstruction process is sketched, from the initial point sets to the resulting surfaces. From the last step the whole procedure can be iterated, even adding additional sedimentary layers and faults, as will be shown in Section 2.

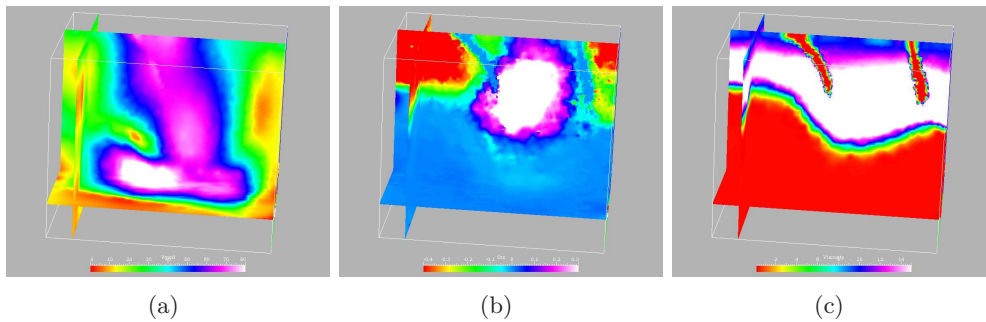


Figure 6: The data post-processing and visualization. The distribution of (a) the module of the velocity, (b) the S_{ZZ} stress component and (c) the viscosity, on a significant section.

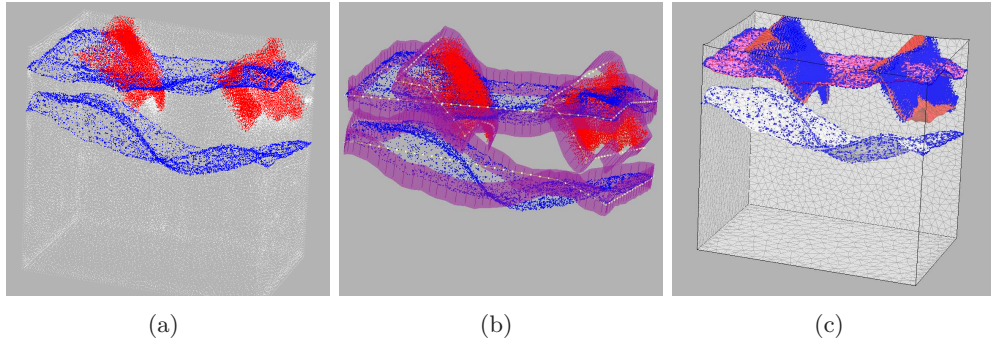


Figure 7: The surface reconstruction sequence. (a) The initial complete dataset (white), with horizon (blue) and fault (red) points clouds. (b) The surface nodes are constrained to move along an optimized fixed shooting direction; if necessary it can be easily edited in the scripts. (c) The reconstructed surface is a balanced compromise between surface smoothness and data fitting (in blue the control points are highlighted), that can be adjusted by the modeler intervention.

2 Another application: a diapir growth

The procedure we propose can handle complex geometries. In the previous Section we presented our workflow applied to a multi-faulted system. We illustrate now the modeling and the reconstruction of a salt diapir in a stratified sedimentary basin (see Figure 8). The dimension of the region we consider are $8.9 \times 8.7 \times 7.2$ km. We also give an example of inverse structural modeling, that

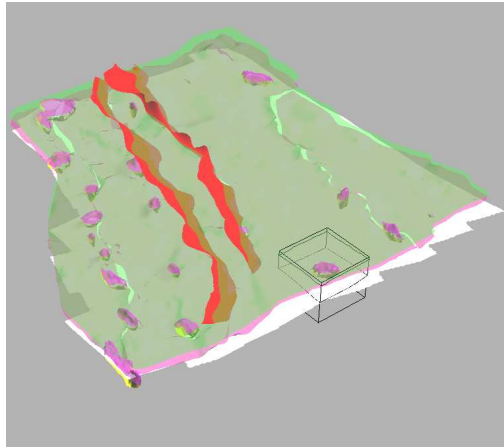


Figure 8: The second case we analyze: a diapir growth in a three-layered sedimentary basin. Diapirs (in magenta and yellow) are displayed to identify the region of interest, but they are more recent than the horizons.

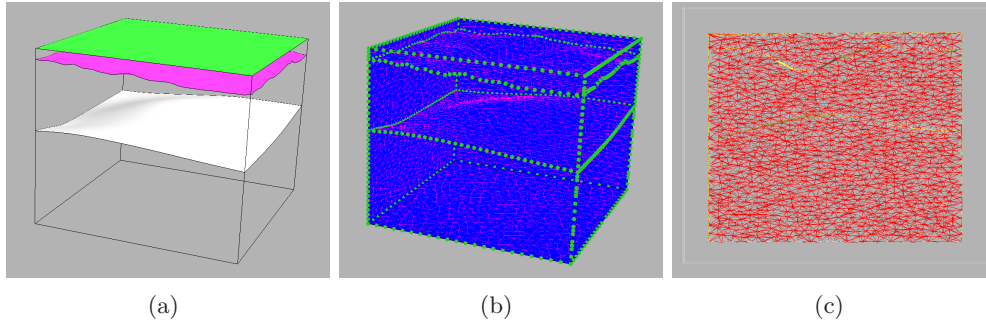


Figure 9: The pre-processing steps. (a) The *Model3d* structural frame: the basement is chosen to conserve the initial salt volume (white surface). (b) The 1D (green points) and 2D meshes. For the latter, different refinement sizes have been fixed for horizons and lateral walls. (c) A section of the *Solid* object showing the 3D internal mesh.

is how the model can be imported, processed and updated for a restart of the simulation of a new evolutionary step on a modified configuration.

The key feature of this application is the reconstruction of the diapir. Hence we will go through the pre-processing phase simply illustrating the results of the steps that have lead to the 3D mesh, that are sketched in Figure 9. The final model is composed of 26586 nodes and 149178 tetrahedra.

In this case we imposed a subsiding speed on the basin. We show in Figure 10 the distribution of the Z component of the velocity, the S_{ZZ} component of the stress, and the viscosity, after a simulation time of 22.29 millions of year. In the velocity plot in Figure 10(a) the rise of the diapir is evident in the region of positive values of the velocity, as well as in the low stress region in Figure 10(b).

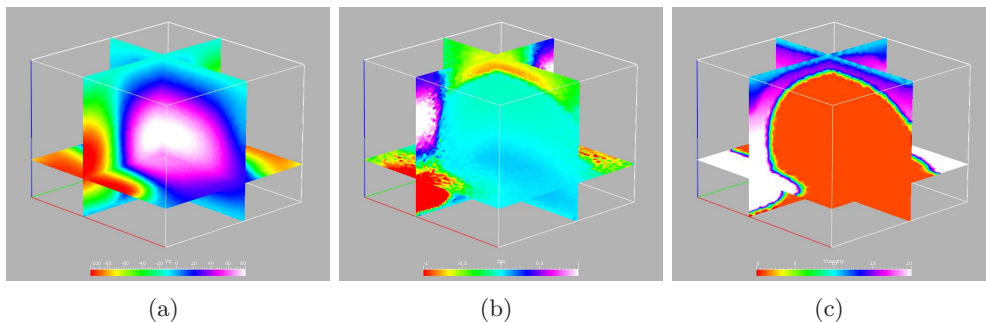


Figure 10: The visualization of some results at a significant cross section. The distribution of (a) the velocity in the Z direction, (b) the S_{ZZ} component of the stress, (c) the viscosity.

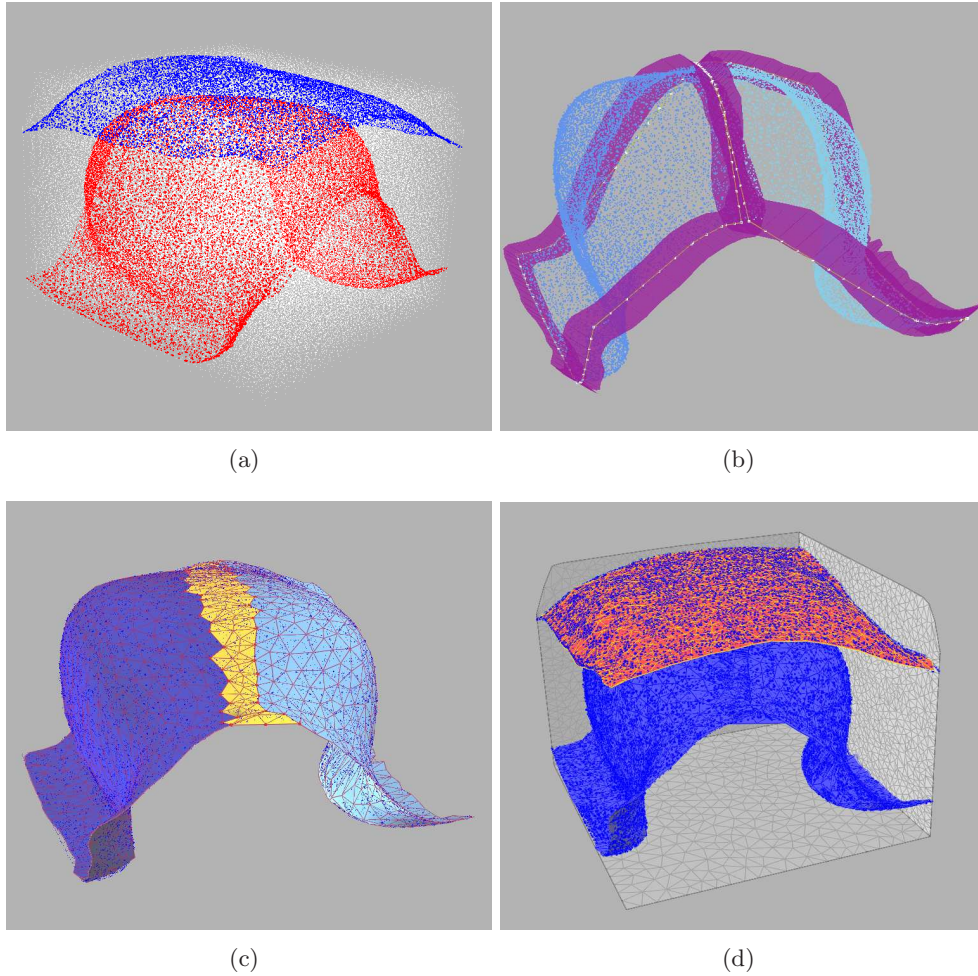


Figure 11: The diapir reconstruction. (a) The mesh nodes (white) and the horizon datasets (red and blue). (b) The shooting direction is optimized to each half-surface, and so are the constraints (in violet) for points movement. This leads to (c) a correct diapir reproduction, that is completed with a patch (yellow) linking the two half-surfaces. (d) The final set of surfaces: the diapir, the horizon and the boundaries.

Also noticeable are regions of descendant velocity and high stress surrounding the diapir.

The generalization to the managing of complex geometries reflects in a more marked modeler intervention, as regards the post-processing phase of surface reconstruction. This is principally due to the behaviour of the available tools, that requires some expedients to correctly reproduce geometries like that of a diapir. Such a shape in fact can not be represented by a single-valued function,

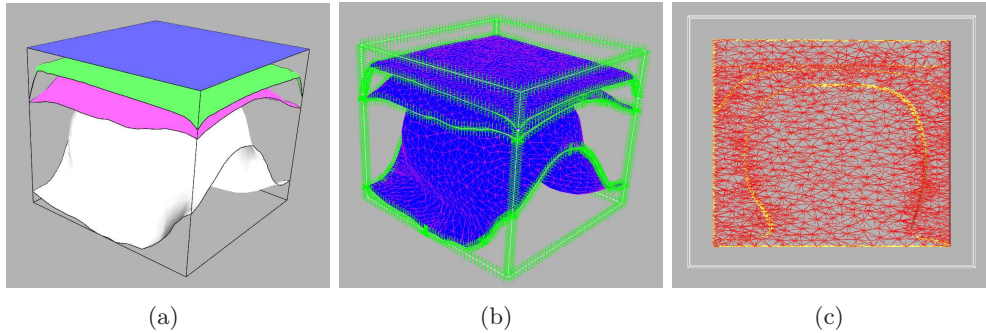


Figure 12: The updated model. In addition to the updated horizons, a new layer and the corresponding horizon (blue) have been added on the top.

and this would lead to errors in the points re-projection onto the approximating surface. The point set must be then divided into two convenient parts, and the automatic reconstruction process must be applied twice. This yields to two discretizing surfaces, as shown in Figure 11(b). Finally, to give continuity to the representation these are connected by a patch, that is fitted to the data points for the sake of accuracy.

Once the surfaces have been reconstructed, it is possible to start again with the pre-processing workflow and create a new model for the following simulation step. In our case, in addition to the modified horizons, we consider an additional layer on the top, that is added to the model simply by including the corresponding horizon in the structural modeling. In Figure 12 the updated configuration is illustrated. By choosing the same meshing parameters of the previous model, the grid definition can be approximately conserved, and hence the overall accuracy. The number of nodes of the updated model is 29562, and the tetrahedra are 124184.

Conclusion and future works

The structural modeling we proposed aims at providing a general direct and inverse procedure for sedimentary basin modeling and restoration data visualization. Starting from horizons and faults surfaces the pre-processing procedure supports the modeler in building a three-dimensional model of a stratified sedimentary basin, with the capability of handling topologically complex geometries such as faults and diapirs. The model is then enriched with additional properties and described with a volumetric tetrahedral mesh for numerical simulations. The post-processing procedure is able to load, process and visualize data coming from a dynamic solver, and to reconstruct model surfaces for configuration updates and simulation restarts, by means of CliCommands scripts. All these steps can be edited by the user and performed in GOCAD through a fully automatic

procedure.

The proceedings have been applied successfully to two significant real cases, a multi-faulted system and a diapir growth in a multi-layered sedimentary basin. The results illustrates the modeling capabilities and the processing possibilities the procedures offer to the modeler.

Ongoing works regard the improvement of the mesh generation process in GOCAD, including a refinement strategy localized to fault regions, to optimize the number of nodes and elements with respect to a specific local resolution. As regards the post-processing, a step forward is the development of a GOCAD user-friendly wizard-based graphical interface to simplify the scripts run and the parameter setting. This goes towards a complete and easier control for the user of the whole process, still maintaining the automatic features that are essential in speeding up the data process and analysis.

References

- [1] S. Marshak and N. Woodward, “Introduction to cross-section balancing”, *In: S. Marshak and G. Mitra, Editors, 1988. Basic Methods of Structural Geology, Prentice Hall*, pp. 303–332, 1988.
- [2] B. J. P. Kaus and Y. Y. Podladchikov, “Forward and reverse modeling of the three-dimensional viscous Rayleigh-Taylor instability”, *Geophysical Research Letters*, vol. 28, pp. 1095–1098, Mar. 2001.
- [3] A. Ismail-Zadeh, I. Tsepelev, C. Talbot, and A. Korotkii, “Three-dimensional forward and backward modelling of diapirism: numerical approach and its applicability to the evolution of salt structures in the pricaspian basin”, *Tectonophysics*, vol. 387, no. 1-4, pp. 81 – 103, 2004.
- [4] F. Lepage, “Triangle and tetrahedral meshes for geological models”, *22nd Gocad Meeting Proceedings, Nancy, France, 2002*.
- [5] P. Muron and J.-L. Mallet, “3d balanced unfolding: the tetrahedral approach”, *23rd Gocad Meeting Proceedings, Nancy, France, 2003*.
- [6] F. Lepage and J.-L. Mallet, “Filling 3d geological models with nice tetrahedra honoring boundaries”, *21st Gocad Meeting Proceedings, Nancy, France, 2001*.
- [7] A. Liu and B. Joe, “Quality local refinement of tetrahedral meshes based on bisection”, *SIAM Journal on Scientific Computing*, vol. 16, no. 6, pp. 1269–1291, 1995.
- [8] J.-L. Mallet, “Discrete smooth interpolation”, *ACM Trans. Graph.*, vol. 8, no. 2, pp. 121–144, 1989.
- [9] J.-L. Mallet, “Discrete smooth interpolation in geometric modelling”, *Computer-Aided Design*, vol. 24, no. 4, pp. 178–191, 1992.

MOX Technical Reports, last issues

Dipartimento di Matematica “F. Brioschi”,
Politecnico di Milano, Via Bonardi 9 - 20133 Milano (Italy)

- 17/2009** M. LONGONI, C. MAGISTRONI, P. RUFFO, G. SCROFANI:
3D Inverse and Direct Structural Modeling Workflow
- 16/2009** G. ALETTI, C. MAY, P. SECCHI:
A functional equation whose unknown is $P([0; 1])$ valued
- 15/2009** S. PEROTTO, A. ERN, A. VENEZIANI:
Hierarchical local model reduction for elliptic problems I: a domain decomposition approach
- 14/2009** L. BEIRÃO DA VEIGA, M. VERANI:
A posteriori boundary control for FEM approximation of elliptic eigenvalue problems
- 13/2009** E.MIGLIO, A. VILLA:
A mathematical derivation of compaction and basin models
- 12/2009** S. BADIA, A. QUAINI, A. QUARTERONI:
Coupling Biot and Navier-Stokes equations for modelling fluid-poroelastic media interaction
- 11/2009** L. FORMAGGIA, A. VILLA:
Implicit tracking for multi-fluid simulations
- 10/2009** P. ZUNINO:
Numerical approximation of incompressible flows with net flux defective boundary conditions by means of penalty techniques
- 09/2009** E. AGOSTONI, S. SALSA, M. PEREGO, A. VENEZIANI:
Mathematical and Numerical Modeling of Focal Cerebral Ischemia
- 08/2009** P.F.ANTONIETTI, P.HOUSTON:
An hr-adaptive discontinuous Galerkin method for advection-diffusion problems